Microelectronic Engineering 163 (2016) 110–114

Contents lists available at ScienceDirect

Microelectronic Engineering

journal homepage: www.elsevier.com/locate/mee

Fabrication of inverted pyramidal pits with Nano-opening by laser interference lithography and wet etching

Baogang Quan *, Zehan Yao, Weijie Sun, Zhe Liu, Xiaoxiang Xia, Changzhi Gu, Junjie Li

Beijing National Laboratory for Condensed Matter Physics, Institute of Physics, Chinese Academy of Sciences, Beijing, 100190, China

ARTICLE INFO

Article history:
Received 29 March 2016
Received in revised form 7 June 2016
Accepted 20 June 2016
Available online 21 June 2016

ABSTRACT

In this work we demonstrate a fabrication process for three-dimensional (3D) container, which is composed of inverted pyramidal pit (IPP) and a cap with nanosized opening fabricated by combining laser interference lithography and anisotropic wet etching processes. The advantages of this method lie in the tunable volume of the pyramidal pit and the diameter of the nano-opening, and its wafer-scale fabrication process. To demonstrate the optical properties of this 3D container, Au film was deposited on the structure through nanosized opening to form a 3D plasmonic nanostructure including above Au hole-arrays and under Au inverted cone. A blue-shift of the absorption dip with the increasing of Au film thickness was observed by study the reflection spectra of 3D plasmonic nanostructure.

© 2016 Elsevier B.V. All rights reserved.

1. Introduction

Periodic three-dimensional (3D) micro- or nano-structure array is of great importance in a wide range of applications, from photonics to biotechnology [1–6]. Anisotropic wet etching of single crystalline silicon is most widely used method for high quality 3D micro-/nanostructures. Kim et al. used silicon anisotropic wet etching on silicon-on-insulator wafers to fabricate nano-sized channels to stretch random coiled DNA, which is a simple, cost-effective, and reproducible solution for the fabrication of nanochannels [5]. Very recently Schurink et al. fabricated 3D silicon sieves by means of corner lithography, which is a combination of double-side photolithography and wet etching in solutions of TMAH and KOH etchants respectively, as hydrodynamic cell capture devices [6]. Inverted pyramidal pit (IPP) is one of the basic structures of the anisotropic etching in a (100) single crystal silicon wafer using grid mask with feature size of micron order [7]. IPPs were used as templates for self-assemble of colloidal nanoparticles as photonic crystals [8]. When combined with dry etching, it can form 3D structures with nanosized structures. Deng et al. developed a method to fabricate nanohole array on the dip of inverted pyramid [9]. The inverted pyramidal structure is a kind of typical 3D structure that can be widely used in many fields. However, until now all the reports concern on the open and uncovered inverted pyramidal structure, which may be a limitation for its further potential applications in biochemistry field. Therefore, once a 3D container array which is composed of IPPs and caps with nanosized opening has been fabricated, it could be a new type of 3D submicron structure with potential applications in optics and biochemistry fields.

The scaling-down of dimensions of 3D structures to submicron and nanometer is a trend for their applications in fields of photonics and biotechnology. Reproducibility, throughput rate, reasonable cost, and flexible design are several of the criteria to be addressed in the practical fabrication of nanostructures especially for 3D structures. Recently Cataldo et al. developed a fabrication strategy of combining of low cost colloidal nanolithography with shadow mask lithography to fabricate large area metal nanostructures as infrared absorption substrates [8]. The shortage of this technique is that they are not suit for fabrication of periodic 3D structures. Electron beam lithography (EBL) method can generate well-ordered pattern with nanometer feature-size, but its serial scan mechanism is too slow and hence not suitable for high-volume application. Moreover, EBL and projection optical lithography are not suitable for the applications mentioned above because such high resolution patterning technique is expensive and not widely available. Amongst the nanopattering techniques available nowadays, laser interference lithography (LIL) and Talbot lithography have attracted much attention because they are well suited to fabricate periodic structures, such as photonic crystals, plasmonic nanostructures, and biomedical sensors [10]. LIL is a widely used patterning technique for exposure of periodic nanostructures on a photoresist layer with two or more coherent light beams, providing a facile, cost effective, and maskless process suitable for large area patterning [11–14]. Coherent diffraction lithography (CDL) [15] is another lithography technique based on the interference of beams diffracted from the periodic pattern on a mask, which can eliminate the edge roughness of the pattern on the mask

* Corresponding author.

http://dx.doi.org/10.1016/j.mee.2016.06.016
0167-9317/© 2016 Elsevier B.V. All rights reserved.

[16]. Solak et al. developed displacement Talbot lithography (DTL) [17, 18] using the Talbot effect [19]. Although the CDL and DTL techniques have the ability to fabricate subwavelength structures, the need of sub-micron mask prevented its practical use for high throughput fabrication of nanostructures in our present work.

Herein, we present a novel approach for fabricating 3D submicron container array with nano-opening by combining LIL with anisotropic etching of silicon. The overall size of the IPP is of submicron, and it is covered with a SiN_x film with nano-sized opening. The advantages of this method lie in the tunable volume of the pyramidal pits and the size of the opening, and its wafer-scale fabrication process. There are many interesting applications of inverted pyramidal pit arrays, such as chemical nanoreactor, 3D plasmonic structure coated by noble metal, surface enhanced Raman scattering substrate, and structures for biomedicine research. In the end of this work, Au films of different thickness were deposited on the 3D submicron containers to study the reflection properties of periodic plasmonic nanostructures.

2. Experimental details

The array of IPP with nano-opening cap was fabricated by a combining of LIL and anisotropic wet etching process. The new method can conveniently fabricate large area of sub-micron IPP arrays with nano-opening cap. The fabrication processes are illustrated schematically in Fig. 1. Single-side polished n-type (100)-oriented silicon substrates with a resistivity of 10–20 Ωcm were used for the anisotropic wet etching of the 3D nanostructures. A 60 nm thick SiN_x was deposited on the substrate using plasma enhanced chemical vapor deposition, which acted as a masking layer during anisotropic etching (Fig. 1a). The silicon nitride layer used in this work was deposited with an Oxford Plasmalab System 100 PECVD reactor (Oxford Instrument Co., UK).

To fabricate large area sample with array of IPP, we choose LIL as the pattern definition technique and more details are provided elsewhere [13]. Its advantages over other lithography techniques lies in that it can fabricate well-ordered period nanostructures over a large area with a low cost system. The silicon wafer with a SiN_x film of 60 nm was cleaned and coated with a layer of 120 nm *AR*-P 5350 photoresist (1:5 diluted, ALLRESIST GmbH). Then, the sample was exposed in our home build LIL system with a 325 nm wavelength helium cadmium laser source (IK Series, Kimmon Koha Co. Ltd., Japan; model: IK3301R-G) for the first time to form one dimensional grating. We then exposed the photoresist again using the same sample rotated by 90° to create photoresist dot array, as shown in Fig. 1b. To ensure a clear surface for Ni deposition, the samples were cleaned by oxygen plasma in a Plasmalab 80 plus reactive ion etching system (RIE, Oxford Instrument Co., UK) for 30 s to remove the residual photoresist.

The sample was thereafter coated with a layer of 20 nm Ni film by electron beam evaporation (Fig. 1c). Ni was selected as the dry etching mask because of its good adhesion with silicon nitride substrate and its high etching selectivity to SiN_x. Followed with a lift-off process, we got a Ni mesh with nanosized hole array (Fig. 1d). We then etch the unprotected area of silicon nitride using a RIE reactor. The RIE process was performed on with the RF frequency of 13.56 MHz. The sample was cleaned with 10% nitric acid deionized water solution for 5 min at room temperature to remove the Ni mesh from the surface. The pattern of silicon nitride with nanosized hole array formed in this step served as a mask for the anisotropic etching of the underlying silicon in KOH solution (Fig. 1e). The anisotropic wet etching was carried out in a 25 wt% KOH solution with added IPA at 80 °a (Fig. 1f). Use of 25 wt% tetramethyl ammonium hydroxide (TMAH) as an alternative etchant for silicon anisotropic etching is advantageous because TMAH is less toxic than KOH. Finally by control the wet etching time, 3D submicron container array composed of IPPs with nano-openings was obtained as shown in Fig. 1g.

To study the optical application of the 3D submicron structures, we fabricated 3D plasmonic nanostructures by directly deposition gold on the as fabricated samples. A 3D container array sample was rinsed by acetone, methanol, and de-ionized water sequentially, and then dried by nitrogen gas flow. Gold films with different film thickness (10, 20, 30, 40, 50, and 60 nm nominal thicknesses) were deposited on the samples using an electron beam evaporation system to fabricate 3D plasmonic nanostructures. The nominal thickness was measured by a quartz crystal balance connected to a thickness monitor. Reflection measurement of 3D plasmonic nanostructures was carried out at room temperature

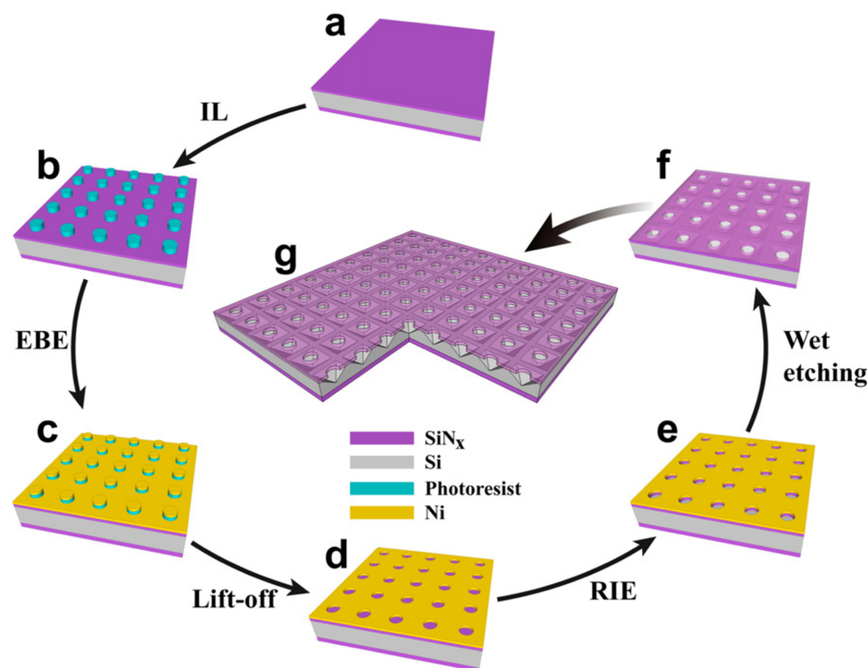

Fig. 1. Schematic view of the fabrication process of 3D container which is composed of IPP array with nano-openings. (a) Si wafer coated with a 60 nm thick SiN_x film by PECVD method. (b) Periodic photoresist dot array on SiN_x by LIL. (c) A 20 nm of Ni film was deposited on the surface by electron beam evaporation. (d) Lift-off process to get a Ni mesh as hard mask for RIE etching. (e) The pattern of nano-hole array on Ni was transferred to SiN_x film by RIE dry etching. (F) Anisotropic wet etching of the single crystal (100) Si to form a 3D container array. (g) A cross-sectional view of 3D submicron containers.

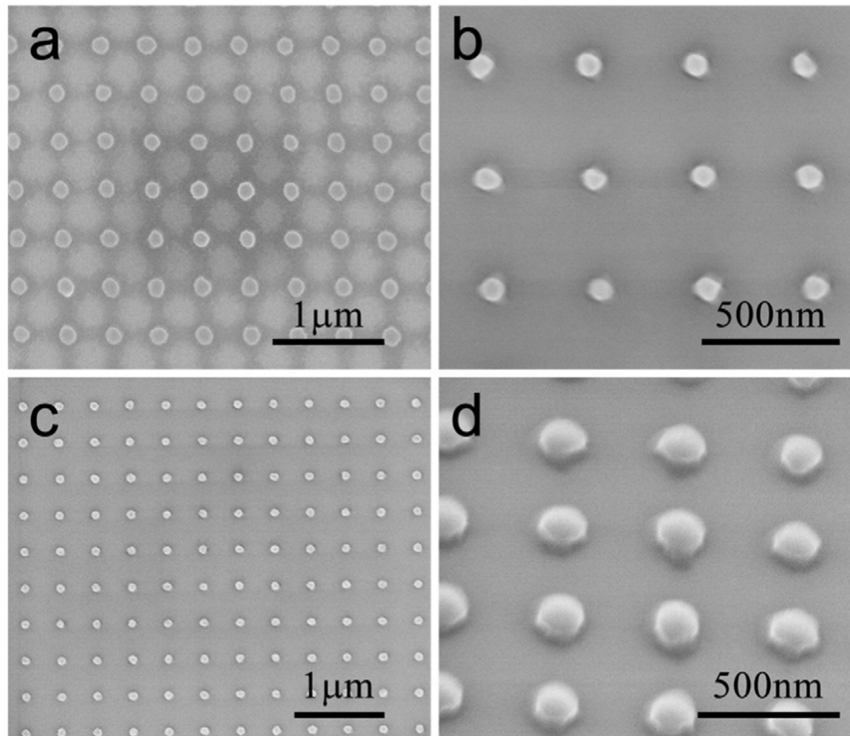

Fig. 2. SEM images of photoresist dot arrays with different periods. (a) SEM image of photoresist dot array with 500 nm period. (b) SEM image of the same sample with (a) but with a 30 s of oxygen plasma treatment. (c) SEM image of photoresist dot array with 400 nm period. (d) Cross-sectional view SEM image of photoresist dot array with 400 nm period after oxygen plasma treatment.

using a home-made integrated microscope-spectrometer system. The system includes a spectrometer iHR-320 from HORIBA Jobin-Yvon, an OLYMPUS BX51 microscope, and a two-channel detector. A 100× objective lens was used to collect the far-field light, and then the light was dispersed by monochromator with 3 selectable gratings of the iHR-320 spectrometer and then detected by a two-channel detector.

The inspection of the IPP structure was carried out by a field emission scanning electron microscope (SEM) of FEI Dual Beam 235 focused ion beam system (FEI Company, USA). The planar morphology of IPP with nano-opening was characterized with tapping mode atomic force microscopy (AFM, Agilent 5500 coupled with VISTA T300R probe).

3. Results and discussion

3.1. Characterization of the fabrication process

Fig. 2a shows the SEM image of photoresist dot-array after interference lithography. Oxygen descum process was carried out to afford a clean wafer surface with no photoresist residue left on the surface. From Fig. 2b we can see that the surface of the sample after an oxygen descum process is free from any photoresist residue. The importance of the oxygen plasma processing not only lies in the fact that it can clean the sample surface but also in making the shape of resist dot more round. Fig. 2c is the SEM image of photoresist dot array with period of 400 nm, which is different from Fig. 2a of 500 nm by adjusting the LIL angle. Fig. 2d shows the tilted view of enlarged SEM of photoresist dot array with 400 nm period, which also shows the diameter to pitch ratio in Fig. 2c is smaller than that in Fig. 2a. This means that the LIL system we used could fabricate well-ordered periodic dot-array with controllable period and diameter. The diameter of nano-opening can be tuned by modifying the exposure time and developing time. Then we transferred the periodic photoresist pattern to SiN_x by RIE etching with a nickel mask. The nickel mask was intentionally removed from the sample before an anisotropic wet etching step. Finally, with the anisotropic wet etching we got high quality sample with 3D submicron container array.

Fig. 3 presents the etching evolution of 3D submicron container array with period of 400 nm. The red line and black line are the measured depth and width of IPPs with etching time of 60 s, 120 s and 180 s, respectively. From this figure, we can see that the wet etching rate of the IPP is stable. In the dimension of opening structure, it is noted that the size and depth of sub-micron cavities is proportional to the wet etching time. The SEM images of wet etching time of 60 s, 120 s and 180 s are presented in the right side of the figure. Though the mask for wet etching is SiN_x film with circular-shape nanohole,

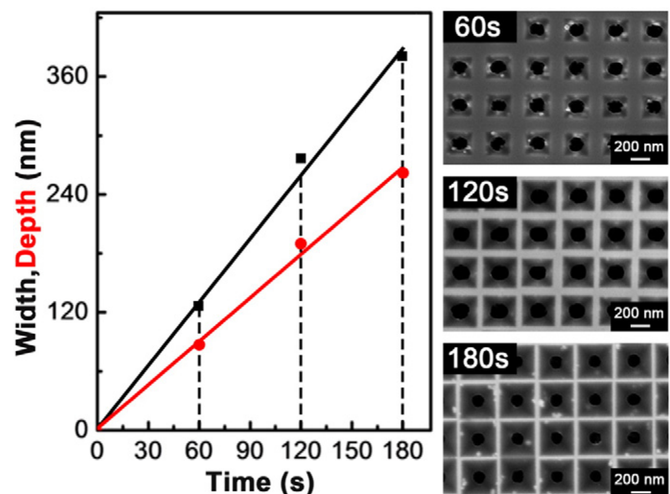

Fig. 3. The curves of the depth (red line) and width (black line) of IPPs with anisotropic wet etching times of 60 s, 120 s and 180 s. Right to the curves are the SEM images of IPP with the etching time of 60 s, 120 s and 180 s, respectively.

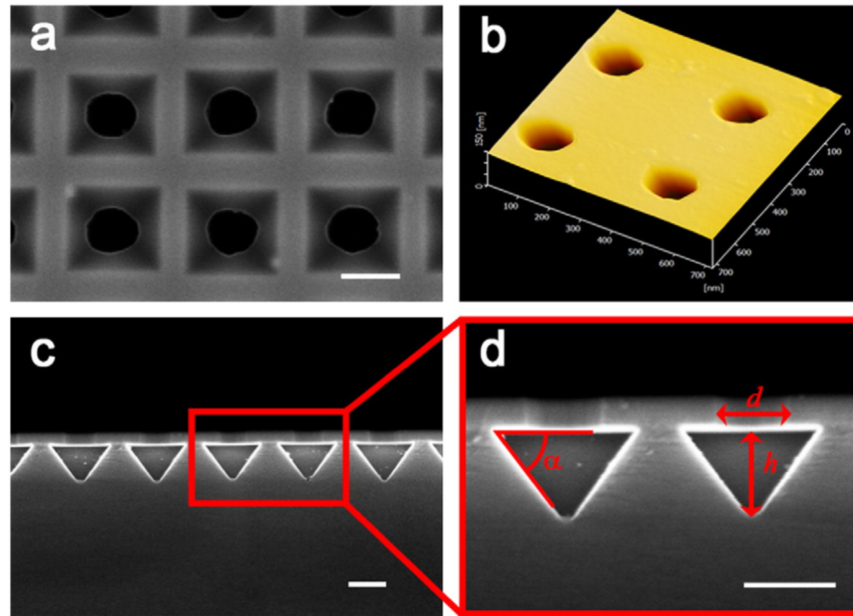

Fig. 4. (a) and (b) are the top-view SEM and AFM images of the 3D container, respectively. (c) Cross-sectional view SEM image of the 3D container and (d) an enlarged image of 3D containers with critical size parameters.

inverted pyramidal pits form a self-aligned array in a perfect manor. Fig. 4a shows the top-view SEM image of an IPP array with nano-openings. Moreover, the flat surface of cap with nano-opening was characterized by AFM (Fig. 4b). From the cross-sectional view of inverted pyramidal pits (Fig. 4c and d), we can see the period of the pit array is about 400 nm, and the diameter of the nano-opening is about 160 nm, the height of the cavity is about 190 nm, and the inclination angle of about 54°. As discussed above, we evaluate that the LIL and anisotropic wet etching are critical processes in the fabrication procedure for the fabrication of 3D submicron container array with controllable nanosized openings. The fabrication techniques, including LIL and anisotropic wet etching, used in our fabrication procedure are well known. However, the conception of the 3D submicron container array with controllable nanosized opening in silicon wafer is original, and has many potential applications in biochemistry and nano-optics fields.

3.2. Reflection measurement of 3D plasmonic nanostructures

To study the optical properties of 3D container sample coated with gold film, we deposited Au film with different thickness on samples with same critical size parameters. Fig. 5 shows the evolution of the reflection spectra of 3D periodic plasmonic nanostructures while the thickness of Au film increasing from 10 nm to 80 nm. And Fig. 5b–e show the cross-sectional SEM images of the 3D plasmonic nanostructures. In Fig. 5a, the reflection intensity increases with the gold film thickness, which is an obvious conclusion in thin film optics that a thicker metal film leads to less transmitted energy and more reflected energy. Besides, the dips in the curves have blue shift from 600 nm to 500 nm with increasing gold film thickness. The dips should be attributed to resonance in the metal holes. On one hand, the optical constant of thin metal film changes gradually with film thickness because of the growth of metal grains, where the volume density and polarizability of metal grains have significant effect on the optical constants [20]. On the other hand, thicker metal film will lead to shrinking of the holes, and the localized surface plasmon resonance on the metal holes has blue shift with the size reduction [21].

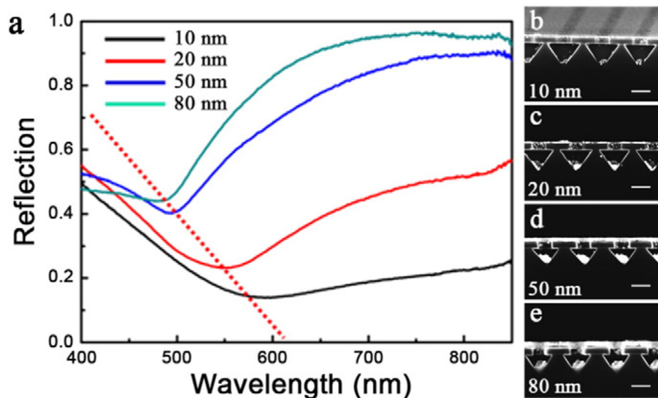

Fig. 5. (a) Reflection spectra of 3D plasmonic nanostructures with Au film thickness of 10 nm, 20 nm, 50 nm and 80 nm, respectively. (b–e) are cross-sectional view SEM images of corresponding plasmonic nanostructures.

4. Conclusions

In conclusion, we have developed a process for the fabrication of 3D micro-container IPPs with precisely controlled volume and size of the opening over a large area. The advantages of this method lie in the tunable volume of the pyramidal pit and the diameter of the nano-opening, and its wafer-scale fabrication process. The reflection spectra of Au coated IPP samples were tested, which show the reflection shift to short wavelength and increase with increase of the thickness of Au film. Therefore it is expected that the IPP structures have many interesting potential applications, such as surface enhanced Raman scattering substrate and micro-/nano-container for biomedicine research.

Acknowledgements

This work was supported by the National Natural Science Foundation of China (grants 91323304, 11174362, 51272278, 11574369, 11574385, 11504414), the Knowledge Innovation Project of CAS (grant No. KJCX2-EW-W02).

References

[1] J.W. Berenschot, N.R. Tas, H.V. Jansen, M. Elwenspoek, Nanotechnology 20 (2009) 475302.

[2] Q.B. Xu, L. Tonks, M.J. Fuerstman, J.C. Love, G.M. Whitesides, Nano Lett. 4 (2004) 2509.
[3] M. Sledzinska, B. Graczykowski, F. Alzina, J. Santiso Lopez, C.M. Sotomayor Torres, Microelectron. Eng. 149 (2016) 41.
[4] S. Matsuo, T. Fujine, K. Fukuda, S. Juodkazis, H. Misawa, Appl. Phys. Lett. 82 (2003) 4283.
[5] S.K. Kim, H. Cho, H.K. Park, J.H. Kim, B.H. Chung, J. Nanosci. and Nanotechn. 10 (2010) 637.
[6] B. Schurink, J.W. Berenschor, R.M. Tiggelaar, R. Luttge, Microelectron. Eng. 144 (2015) 12.
[7] E. Sarajlic, C. Yanmahata, H. Fujita, Microelectron. Eng. 84 (2007) 1419.
[8] S. Cataldo, J. Zhao, F. Neubrech, B. Frank, C.J. Zhang, P.V. Braun, H. Giessen, ACS Nano 6 (2012) 979.
[9] T. Deng, J. Chen, W.H. Si, M. Yin, W. Ma, Z.W. Liu, J. Vac. Sci. Technol. B 30 (2012) 061804.
[10] J. Yang, C. Sauvan, H.T. Liu, P. Lalanne, Phys. Rev. Lett. 107 (2011) 043903.
[11] M.J. Beesley, J.G. Castledine, Appl. Opt. 9 (1970) 2720.
[12] M. Campbell, D.N. Sharp, M.T. Harrison, R.G. Denning, A.J. Turberfield, Nature 404 (2000) 53.
[13] H. Korre, C.P. Fucetola, J.A. Johnson, K.K. Berggren, J. Vac, Sci. Technol. B 28 (2010), C6Q20.
[14] S.C. Lee, S.R.J. Brueck, J. Vac. Sci. Technol. B 22 (2004) 1949.
[15] H. Dammann, G. Groh, M. Kock, Appl. Opt. 10 (1971) 1454.
[16] C. Zanke, M.H. Qi, H.I. Smith, J. Vac. Sci. Technol. B 22 (2004) 3352.
[17] H.H. Solak, C. Dais, F. Clube, Opt. Expr. 19 (2011) 10686.
[18] H.H. Solak, C. Dais, F. Clube, L. Wang, Microelectron. Eng. 143 (2015) 74.
[19] W.H.F. Talbot, Philos. Mag. 9 (1836) 403.
[20] R.W. Cohen, G.D. Cody, M.D. Coutts, B. Abeles, Phys. Rev. B 8 (1973) 3689.
[21] A. Degiron, H.J. Lezec, N. Yamamoto, T.W. Ebbesen, Opt. Commun. 239 (2004) 61.